Monitoring strain development of soil slope using distributed optical fibre sensor

IOP Conf. Series: Materials Science and Engineering **527** (2019) 012027 doi:10.1088/1757-899X/527/1/012027

Monitoring strain development of soil slope using distributed optical fibre sensor

Dayangku Salma bt Awang Ismail[1,2*], Assoc Prof Ir Dr Azman b Kassim[2], Assoc Prof Ir Dr Hisham b Mohamad[3], Assoc Prof Dr Ahmad Safuan b A Rashid[2], Aliff Ridzuan b Bunawan[2]

[1]Universiti Malaysia Sarawak,
[2]Universiti Teknologi Malaysia,
[3]Universiti Tekonologi PETRONAS.

*Corresponding author e-mail: aidsalma@unimas.my

Abstract. Rainfall infiltration is well-known as one of the important factors that lead to slope failure in tropical areas such Malaysia because it's significant fluctuation of pore water pressure due to monsoon seasons. In this paper, a distributed sensing optical fibre system named Brillouin Optical Time Domain Analysis (BOTDA) is used to monitor the strain development of a laboratory soil slope model. The aim of study is to determine the plane failure of a residual soil slope under rainfall infiltration and subsequent loading impact using BOTDA technology. A soil slope model was constructed from Malaysian residual soil slope and tested under various rainfall infiltration patterns and sequential loadings. A continuous ribbon optical fibre has been directly embedded in the soil slope to measure the soil strain. The paper only presented on soil strain response due to rainfall infiltration and relations to the pore pressure development within the finite slope. From the experiments, it has been observed that the optical fibre has been able to capture soil strain during infiltration which proven the sensitivity of optical fibre to measure soil strain. The maximum strain observed was about 850 microstrain (με) which occurred at the third layer of slope height (L1) at 8-hour of infiltration. After 24-hours of infiltration, the strain was observed to be constant for all layers; Layer 1 (L1) = 302 με, Layer 2 = 210 με and Layer 3 (L3) = 190 με in which the whole sample was clearly seen in a fully saturated condition and the negative pore pressure has remained constant throughout the depth.

1. Introduction

Research studies in rainfall-induced landslides focused on the response of pore water pressure to slope stability condition and how it has affected the matric suction distribution in a soil mass. The subject matter was a longstanding research which has been explored through field and laboratory scale by many scholars especially for those in unsaturated soil mechanics area. (1 - 8). However, none of them discussed on deformation of slope regards to suction variation in slope. Alonso et al. 2003 (3) and Sasahara et al. 2014 (4) have been initiated studies concerning to pore pressure variation and soil deformation inside a slope during rainfall infiltration. Recent research by Leung et al. (5) performed a field monitoring related to the behaviour of deformation characteristics of soil slope due to wetting and drying event (pore water pressure variation) and its response to stress mobilisation in slope. However, the current slope deformation measurement methodologies are still not convincing enough due to many inaccuracies in their predictions.

The present slope movement monitoring scheme like inclinometer, multi-point extensometer and total stations are basically predicting deformation in a point monitoring manners. Therefore, it is quite impossible to obtain a so called continuous displacement profile and these data is very essential to predict deformation of a slope with a complex geological profile (6). Pei et al., 2011 (7) had started on integrating Fibre-Bragg Grating sensor and inclinometer to measure slope movement and also had obtained the displacement values from the strain results of a series of rods with FBG sensors. Then, Huang et al., 2012 (8) and Tan et al., 2013 (9) have started the uses of optical fibre as a sensing system for rainfall infiltration. They have used FBG technology to measure pore-water pressure during rainfall infiltration and relates to the stability of slopes. However, the needs of measuring ground displacement to predict landslides also important rather than only relying on the pore-water pressure readings in soil slope.

About a decade, few researchers have had started to discover on the practices of distributed optical strain sensing system to monitor slope movement; for instance Shi et al., 2008 (10), Wang et al., 2009 (11), and Olivares et al. 2009 (12) have proven the technology was more beneficial compared to other optical fibre in monitoring slope movement. Shi et al. 2008 had used BOTDR system to monitor the strain mobilisation for lattice beam, anchor bolt, slide-resistant pile and retaining wall etc. and had emphasized on the importance of layout and method of installation of the optical fibre (10). Wang et al., 2009 (11) had set-up different types of optical fibre which had been embedded directly in the slope model and had concluded that irregular strains were observed during the incremental loading stage which indicated a progressive deformation of the slope before a failure. While Olivares et al. 2009 (12) had constructed a 40 degree inclination of unsaturated granular soils flume and was instrumented with several monitoring devices covered tensiometer, time domain reflectometry (TDR) device, rain gauge, particle image velocimetry (PIV) system and distributed optical fibre sensors. The optical fibre cable was installed at the longitudinal sections of the flume and a 1cm by 1 cm square geo-grids were mounted to the fibre to avoid the occurrence of relative displacement between the geo-grids and adjacent soil.

The research work criteria done by Wang et al., 2009 (11) and Olivares et al. 2009 (12) have been adopted to the recent study to investigate the progressive strain development using distributed optical fibre technology. The arrangement of optical fibre layering was adopted from Zhu et al., 2014a (14) and several research works mentioned in this paper.

2. Materials and Method

A small model test of finite soil slope was constructed in a chamber of 1.0 m length, 0.3 m width and 0.8m height. The chamber body is made from acrylic glass supported with steel frame. Three of the glass panels were pre-drilled with 31 holes to allow access for placing remote positioning tensiometers whereas the one side of the wall without holes is required for Particle Image Velocimetry test (PIV). The material used in this study is classified as residual soil (Grade VI) type and categorized as sandy Silt. The soils were obtained within the Universiti Teknologi Malaysia (UTM) premises which is located in front of P16 block of Electrical Engineering. Summary of soil model physical properties are tabulated as in Table 1. The soil properties were obtained in accordance to British Standard Soil Classification.

Table 1. Soil Model Properties.

Description	Grade VI – Residual soil	
Composition	Gravel (%)	0
	Sand (%)	33
	Silt (%)	34
	Clay (%)	33
Moisture content	42	
Liquid Limit	59.3	
Plastic limit	31.9	
Plasticity index	27.4	

Specific gravity, G_s	2.65
Saturated Coefficient of Permeability, k_{sat}(m/s)	5.00×10^{-7}
Bulk density, ρ_b(Mg/m3)	1.74
Dry density, ρ_d(Mg/m3)	1.38
Maximum dry density, MDD (Mg/m^3)	1.42
Optimum moisture content, OMC (%)	31
Effective cohesion, c' (kPa)	7.6
Effective frictional angle, ϕ' (°)	32.1

2.1. Preparation of Artificial Rainfall

The artificial rainfall simulator was designed to reproduce local rainfall infiltration and water distribution within a soil mass. The pumping water flow system is opted for the raining demonstration and five nozzles with 8 inches centre-to-centre were used in this study. The artificial rainfall intensities were obtained and calculated from Intensity-Duration-Frequency (IDF) curve based on Johor Bahru area. Department of Irrigation and Drainage Malaysia Malaysia (2001) has published a polynomial equation for one day (i.e. 1 hour to 24 hours) IDF curve. This equation was contained in Urban Stormwater Management Manual for Malaysia (Manual Saliran Mesra Alam Malaysia), 2006 volume 4. This equation is given as

$$ln({}^{R}I_t) = a + b\ln(t) + c(\ln(t)^2 + d(\ln(t))^3 \qquad [1]$$

where,
$({}^{R}I_t)$= average rainfall intensity (mm/hr) for average recurrence interval (ARI) and duration t
R = Average return intervals (years)
t = Duration (minutes)
a, b, c and d are fitting constants which depends on return period and geo-graphical condition.

2.2. Data acquisition set-up for distributed optical fibre sensor

Prior to test, a baseline configuration of Brillouin spectrum is performed as it will be used to measure the attenuation data along the cable with a certain spatial resolution. The commercial demodulation instrument; OZ Optics' Foresight™ series of fiber optic Distributed Strain and Temperature Sensors (DSTS) BOTDA module was able to reach a spatial resolution of 1 ns, spatial step of 5cm, measuring accuracy of ±2 micron, strain range cover -3% (compression) to +4% (elongation) and maximum measurement is 100km. The pulse width defines the width of probe pulse in nanoseconds (ns) which determine the measurement range or spatial resolution. For instance, a 1ns corresponds to a spatial resolution of 10cm and measurement taken at half of maximum width. The spatial step parameter defines the distance between each point of measurement. As example, a 1ns pulse width able to corresponds with 5cm spatial step and 10cm spatial resolution. In this study, the BOTDA interrogator was set-up to 5ns spatial resolution and 5cm spatial step of measurement to match a total measurement length of 25 m.

The preparation of optical fibre sensor needs a special apparatus named fibre cleaver and a Direct Core Monitoring Fusion Splicer (Figure 1a and Figure 1b respectively) for the splicing process. The splicing process was purposely to join the optical fibre cable and optical connector which then the latter was connected to BOTDA sensing interrogator (Figure 2). The 12-ribbon Fujikura optical fibre was used as the sensing cable because of the design of outer cladding has provided a better surface area compared to other single core optical fibre with circular cross-section which had assisted the strain transfer mechanism to the optical fibre core (refer Figure 3). The strain and temperature dependence of

Brillouin shift, ΔV_b and therefore calibration tests had been performed as to translate the signal (frequency) data to strain or/and temperature readings. Then, the result from calibration tests were used as a configuration set-up parameters of optical fibre before any commencement of testing. The configuration parameters stated in the paper were only for 12-ribbon Fujikura optical fibre cable and any new optical fibre cables to be used are necessarily demanded for a calibration testing so that signal interpretations from the BOTDA interrogator are meaningful for the researchers.

In order to evaluate the strain coefficient, the 3m length strain rig was used with a guiding tracks on the left side. The other side is a fixed clamp and the strained fiber section can be adjusted to maximum length of 1.5m. From the test, the coefficient of strain and temperature represented by 20με/Mhz and about 1 degree Celcius/Mhz respectively. The temperature coefficient is obtained by placing some meters of the optical fibre inside a water bath. The part of cable which inside the water bath was taken as the reference point. The baseline temperature was set up as 23 degree Celsius (tap water) and the water was heated up till 62 degree Celsius. Both strain and temperature coefficient were obtained by evaluating the Brillouin shift frequency according to variation of temperature and strain.

(a) (b)

Figure 1. (a) Direct Core Monitoring Fusion Splicer; (b) Optical Fibre Cleaver.

Figure 2. Fiber Optic Distributed Strain and Temperature Sensors (DSTS) BOTDA Interrogator. (www.ozoptics.com)

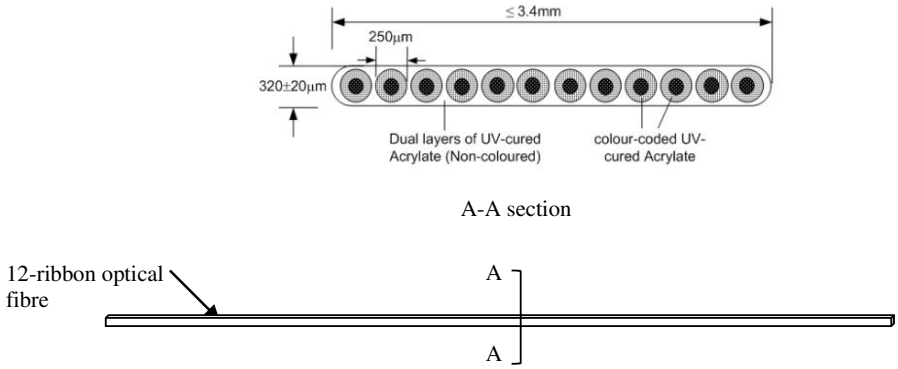

Figure 3. A schematic diagram of sensing fibre (15) (modified from Mohamad 2008).

2.3. Preparation of Remote Positioning Tensiometer

The remote positioning tensiometer used in this study consisted of a porous ceramic cup that has a high air-entry value of 100 kPa. The ceramic cup was featured with a diameter of 6 mm, and a length of 25 mm. A vent tube of 3 m length was used to attach the ceramic cup to the body of tensiometer. A proper calibration of a ceramic cup should ensure it is saturated and the body of tensiometer are free of air bubble. To achieve this condition, the de-aired distilled water is used. The ceramic cup and the vent tube is mounted with a threaded housing on the sidewall. A specially designed connector that fit well into the threaded housing, O ring, and sealing tape has been used to form a good seal at the ceramic cup-tube connection. A pressure transducer was used to replace the vacuum gauge for automated suction measurement. The pressure transducer was manufactured by Soil Moisture Corp., Model 5301-B1. This type of transducer is relatively inexpensive and has a very rapid response time. The pressure transducer has a measuring range from zero to 100 kPa and requires a power supply of 12V–30 V direct-current. The assembly of the tensiometer-transducer formed a tight seal. The other end of the transducer was connected to the CR8x data logger via a signal cable. Each transducer was assigned to an independent channel in the multiplexer of the data logger. The tensiometer-transducer system was able to measure and register pore-water pressures in the soil continuously. Each of the data loggers was calibrated before used in the infiltration tests, as shown in Figure 4.

Figure 4. Calibration of tensiometer acquisition system.

2.4. Construction of Slope Model

A slope model was constructed at slope height of 0.3 m, base height of 0.2 m and 1 to 2 finite slope inclination. An initial soil condition has to be achieved prior to any laboratory testing which as much as possible able to represent the true condition of site suction state. In order to establish the initial condition in a laboratory slope model, the density of soil model was determined to relate the actual site condition. Firstly, the quantity of soil required to a total height of 500-mm soil slope was computed and its remoulding water content was derived from residual water content of the soil. The relationship of residual water content, θ_{res} and water content, w is presented in Equation 2 (16). The density of test soils was then calculated and 5 series of horizontal soil layers with a thickness of 100 mm each is produced by tamping the soil-water mixed in the model chamber until the desired height was obtained. The initial condition of about 30kPa should be attained in the model chamber and repetition procedure of tamping the soil layer was claimed to create a homogenous soil mass in the test chamber.

$$\theta = w\frac{\rho_d}{\rho_w} \qquad [2]$$

The optical fibre cables were placed in horizontal direction perpendicular to surcharge load position. The three layers of sensing cables were laid at depths of 0.1m, 0.2m and 0.3m from crest and represented as L3, L2 and L1 respectively (Figure 5). The optical fibre was inserted in the model in a longitudinal direction in S-shape formation. The Brillouin shift dv_b or frequency difference for Brillouin-based optical fibre sensors are depended on the strain $d\varepsilon$ and temperature, dT. The common methods to eliminate temperature effects in BOTDA measurements are free loose section, distributed temperature sensor, the Landau-Plazcek ratio and loose-tubed cable (17). For the testing, the free loose section is chosen due to its simplification or straightforward technique. An important assumption made when using this method is that temperature and strain section fibres have the same temperature at all times. In other words, the expansion/ contraction of the cable due the temperature must be equal in both of the sections.

Figure 5. Arrangement of optical fibre layout.

Figure 6 illustrates the two dimensional orthographic drawing of optical fibre arrangement inside soil slope. The optical fibre were arranged inside the soil in longitudinal direction; parallel to the length of slope and it was in of S-shaped formation. The layering of optical fibre inside the soil mass was followed by tamping a 100mm thickness of soil on top of it and was done repeatedly for two times till the final layer at crest. Total height of slope is 300mm. When the layering was finished, every staggered edges of the three compacted layer were trimmed to acquire slope formation; either it was 27 or 45 degree inclination. Finally, both ends of optical fibre were connected to the BOTDA interrogator to start the testing. For the incremental surcharge, the load cell and the pneumatic cylinder were firstly calibrated so that the reading are meaningful and correct. The load cell was connected to the TML data logger to collect the data automatically during the testing. During the raining event, BOTDA was also been set up to collect strain measurements caused by the water infiltration.

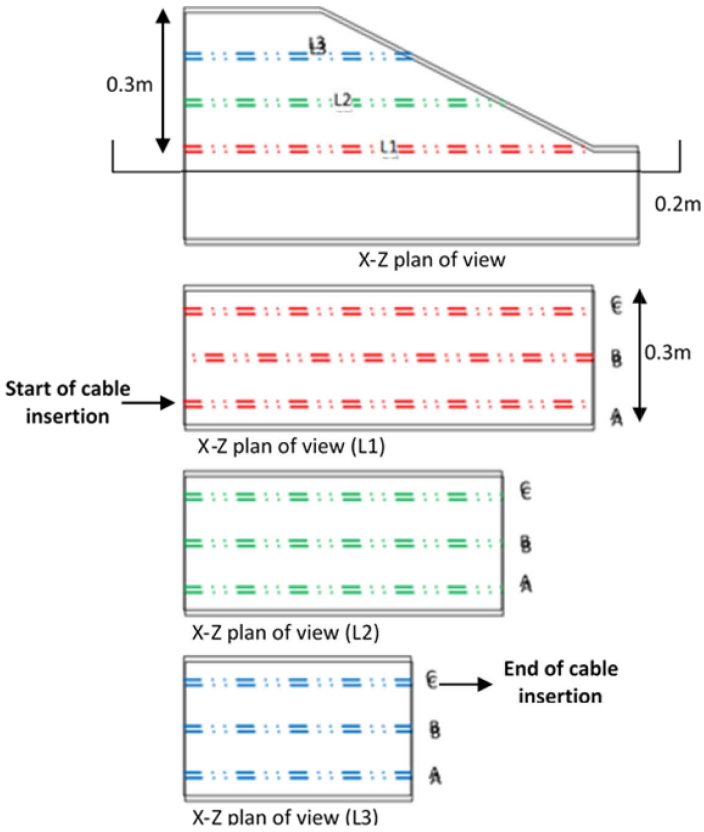

Figure 6. Optical fibre arrangement (i.e 27 degree inclination).

2.5. Pilot laboratory testing

In pilot laboratory testing, two different intensity of rainfall event were demonstrated in order to observe significant changes of strain mobilisation subjected to rain water infiltration. The 1-hour and 2-hour infiltration intensities were about 2.46×10^{-5} m/sec and 1.51×10^{-5} m/sec respectively. In addition, negative pore pressure distribution were observed using mini tensiometer which has been positioned at different locations along the side wall of the slope model. The pore water pressure distributions were monitored from a computer that connected to the tensiometers acquisition system. Three significant locations were identified and were tabulated for further analysis. These locations are the crest, slope face and toe.

As in Figure 7, pore-pressure versus time clearly illustrates on how rainfall pattern was finally decided for the overall laboratory schemes. It appears that for 1-hour and 2-hour rainfall event, the wetting front has reached less than 0.1m depth and did not go further along with depth of slope. At 60minutes of infiltration, it was found that for both 1-hour and 2-hour rainfall patterns had provided not that much different of matric suction readings; -11kPa and -17kPa respectively. This might be occurred due to the same order in rainfall intensity magnitude for both extreme rainfall events (10^{-5} m/sec). Therefore, it was decided that the proceeded laboratory schemes utilized two rainfall patterns (1-hour and 24-hour extreme rainfall) and one controlled test (no rain water infiltration) for the purpose of strain monitoring using optical fibre.

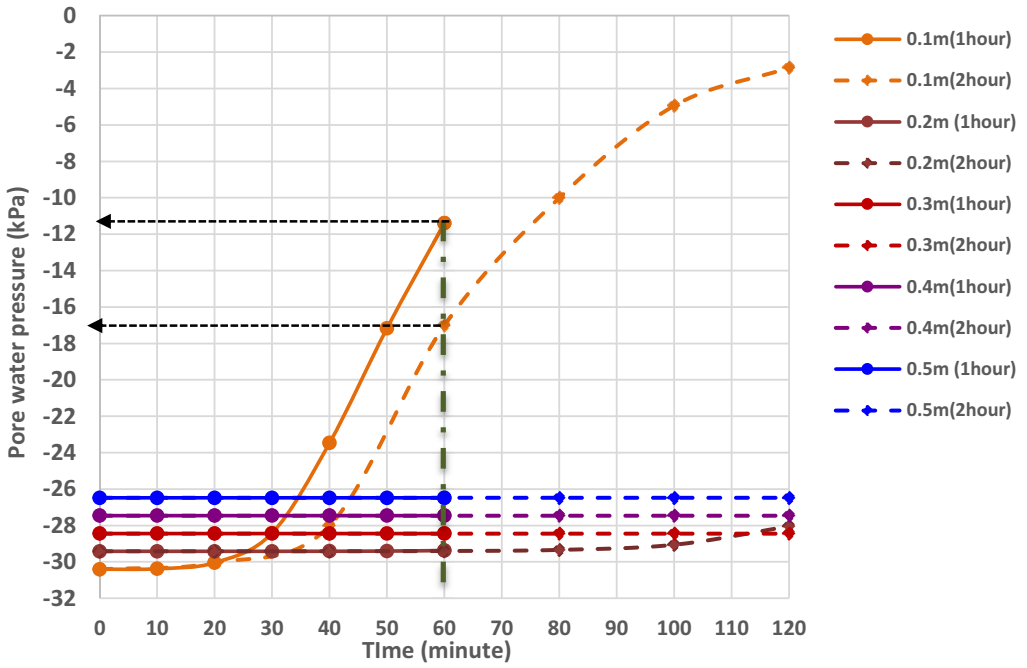

Figure 7.Pore pressure variation with time in homogenous sandy silt.

2.6. The effect of rainfall infiltration to strain distribution

Figure 8 illustrates the strain distribution along the fibre length when the slope was infiltrated with rain water within 24hours. The rainfall intensity for 24 hours rainfall infiltration was simulated as 2.53×10^{-6} m/sec as calculated from the IDF curve. The strain measurement was obtained for every hours to observe the strain development in soil slope due to infiltration. The optical fibre was laid and positioned behind the slope face at different depth. Layer 1 was located at 300 mm depth, Layer 2 and layer 3 were laid at 200 mm and 100 mm depth respectively. At each layer, there were three (3) lines; A, B and C of fibre cable were parallel-arranged to each other at 0.05 m, 0.15 m and 0.25 m from the edge of chamber wall. During the experiment, a surface runoff has been observed at the slope toe for several minutes and finally be able to penetrate into the soil mass. The runoff might be generated due to the ratio of rainfall intensity, I (2.53×10^{-6} m/sec) to saturated hydraulic conductivity of soil, k_{sat} ($\frac{I}{k_{sat}}$) is more than 1 (18,20,21). Therefore, the slope toe was found to be wet compared to the other part of slope model. This phenomena occurred due to the rain water needs some time to penetrate the compacted soil slope because of different rate of permeability. In addition, the matric suction distribution shows a uniform downward progression of infiltrating water throughout the test owing to the homogenous soil system of sandy silt material. The observation of pore pressure readings might be significantly different for a non-homogenous soil system as the existence of breakthrough phenomena between different type of materials (18,19). At the end of experiment, the negative pore pressure has remained constant throughout the depth. This condition has illustrated that slope model has reached a unit gradient which implies an equilibrium condition or known as steady-state condition.

It has been observed that the soil strain was increased proportionally to time. Nonetheless, after 8 hours of infiltration, the strain increment was started to show a constant trend. From the experiment, the maximum strain observed was about 850 microstrain (με) which occurred at the third layer of slope height (L1) at 8-hour of infiltration. Optical fibre sensor at Layer 2 (L2) and Layer 3 (L3) had already reached their maximum and no substantial increment of strain has been seen during the 8-hour infiltration. Besides, the wetting front had advancing up to the third layer at this state (during 8-hour infiltration. Then, the strain readings were still at a constant value at the same location for the subsequent 2 hours, and slowly showed a decrease trend after 11-hours of infiltration until the experiment had completed. After 24-hours of infiltration, the strain was observed to be constant for all layers; Layer 1 (L1) = 302 με, Layer 2 = 210 με and Layer 3 (L3) = 190 με in which the whole sample was clearly seen in a fully saturated condition and the negative pore pressure has remained constant throughout the depth. The optical fibre sensor had illustrated tensile strain during infiltration which means the saturated self-weight of the soil caused the fibre optic to response to its overburden pressure. The chronology of strain increment demonstrates that fibre optic sensors were responsive in accordance to the wetting front advancement from the rainfall event. Within the first two hours, the most upper layer (Layer 3) of fibre optic sensor was responded to the infiltration because the water were slowly penetrated into the soil mass and diminished the matric suction. The saturated soil has caused an extra overburden pressure to the layered optical fibre. The rain water had filled in the voids and had deformed due to water infiltration. As conclusion, the fibre optic sensor was able to measure the movement of soil particles in micro-strain or micro-meter and therefore the optical fibre sensor can be deployed to the geo-structures as a real-time monitoring sensing system.

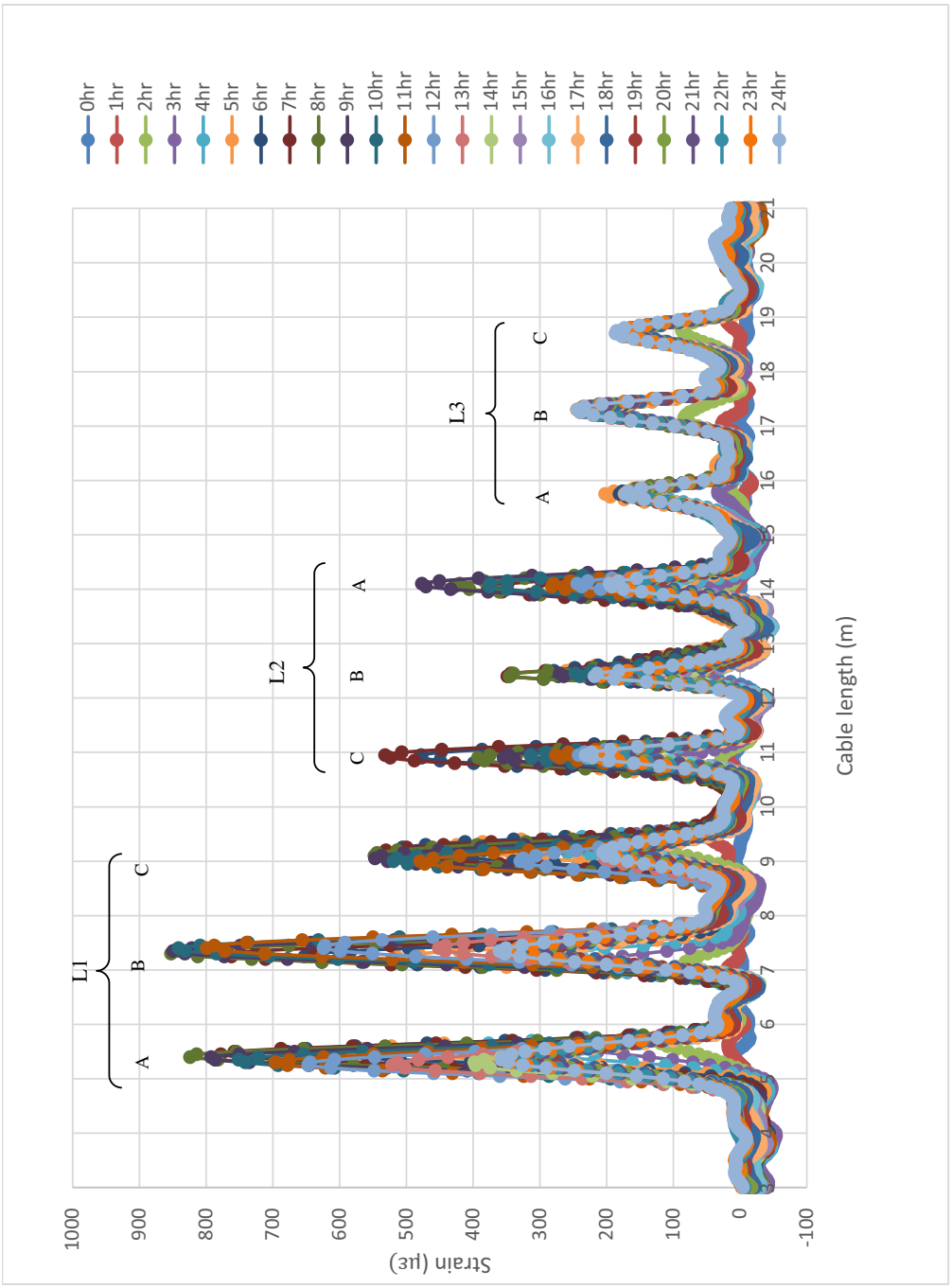

Figure 8. Strain distribution of slope subjected to 24 hours rainfall.

3. Conclusions

A finite slope model with a 1 to 2 slope inclination was instrumented to monitor for both response of suction and strain distribution subjected to rainfall infiltration. The response of suctions were measured with positioning remote tensiometer and strain measurement were obtained using distributed optical fibre sensor. From the experimental work analyses, it can be concluded that distributed optical fibre sensor are sensitive to rainfall infiltration. From the experiment, the maximum strain observed was about 850 microstrain (με) which occurred at the third layer of slope height (L1) at 8-hour of infiltration. Further analysis on how the strain distribution along the optical fibre shall be carried out to study on deformation of slope with respect to variation of pore pressure inside the soil slope.

4. References

[1] Lim TT, Rahardjo H, Chang MF, Fredlund DG. Effect of rainfall on matric suctions in a residual soil slope. Vol. 33, Canadian Geotechnical Journal. 1996. p. 618–28.
[2] Kassim A, Gofar N, Lee LM, Rahardjo H. Modeling of suction distributions in an unsaturated heterogeneous residual soil slope. Eng Geol [Internet]. 2012;131–132:70–82. Available from: http://dx.doi.org/10.1016/j.enggeo.2012.02.005
[3] Alonso EE, Gens a., Delahaye CH. Influence of rainfall on the deformation and stability of a slope in overconsolidated clays: a case study. Hydrogeol J. 2003;11(1):174–92.
[4] Sasahara K, Sakai N. Shear deformation distribution and the variation of pore pressure in a sandy model slope during rainfall. Eng Geol. 2014;170:43–51.
[5] Leung AK, Ng CWW. Field investigation of deformation characteristics and stress mobilisation of a soil slope. Landslides. 2015;55(January).
[6] Zhang C-C, Zhu H-H, Shi B, She J-K. Interfacial characterization of soil-embedded optical fiber for ground deformation measurement. Smart Mater Struct [Internet]. 2014;23(9):095022. Available from: http://www.scopus.com/inward/record.url?eid=2-s2.0-84906225008&partnerID=tZOtx3y1
[7] Huafu Pei, Jianhua Yin HZ and CH. Development and Application of an Optical Fiber Sensor Based In-place Inclinometer for Geotechnical Monitoring Huafu. Geo-Frontiers 2011 © ASCE 2011. 2011;(Dunnicliff 1993):1725–31.
[8] Huang A, Lee J, Ho Y, Chiu Y, Cheng S. Stability monitoring of rainfall-induced deep landslides through pore pressure profile measurements. 2012;52(4):737–47.
[9] Tan DJ, Han B, Li LL, Liu JP. Study on the Application of FBG Technology in Rainfall Monitoring. Adv Mater Res [Internet]. 2013 Mar [cited 2018 Nov 25];668:959–63. Available from: https://www.scientific.net/AMR.668.959
[10] Shi B, Sui H, Zhang D, Wang B, Wei G, Piao C. Distributive monitoring of the slope engineering. 2008;1283–8.
[11] Wang B-J, Li K, Shi B, Wei G. Test on application of distributed fiber optic sensing technique into soil slope monitoring. Landslides. 2009;6(August 2008):61–8.
[12] Olivares L, Damiano E, Greco R, Zeni L, Picarelli L, Minardo A, et al. An instrumented flume to investigate the mechanics of rainfall-induced landslides in unsaturated granular soils. Geotech Test J. 2009;32(2):108–18.
[13] Olivares L, Damiano E, Greco R, Zeni L, Picarelli L, Minardo A. An Instrumented Flume to Investigate the Mechanics of Rainfall-Induced Landslides in Unsaturated Granular Soils. 2009;32(2).
[14] Zhu HH, Shi B, Zhang J, Yan JF, Zhang CC. Distributed fiber optic monitoring and stability analysis of a model slope under surcharge loading. J Mt Sci. 2014;11(4):979–89.
[15] Mohamad H. Distributed Optical Fibre Strain Sensing of Geotechnical Structures. Thesis. Cambridge University; 2008.
[16] Fredlund DG, Rahardjo H, Fredlund MD. Unsaturated Soil Mechanics in Engineering Practice. 2012.

[17] Mohamad H. Temperature and strain sensing techniques using Brillouin optical time domain reflectometry. Proc SPIE 8346, Smart Sens Phenomena, Technol Networks, Syst Integr [Internet]. 2012;8346:83461M. Available from: http://proceedings.spiedigitallibrary.org/proceeding.aspx?articleid=1314666
[18] Kassim A. Modelling the Effect of Heterogeneities on Suction Distribution Behaviour in Tropical Residual Soil. Thesis. Universiti Teknologi Malaysia; 2011.
[19] Yunusa GH. Effect of transport layer system on suction distribution for tropical residual soil slopes gambo haruna yunusa universiti teknologi malaysia. 2015.
[20] Lee LM, Gofar N, Rahardjo H. A simple model for preliminary evaluation of rainfall-induced slope instability. Eng Geol [Internet]. 2009;108(3–4):272–85. Available from: http://dx.doi.org/10.1016/j.enggeo.2009.06.011
[21] Gofar N, Lee LM, Kassim A. Response of suction distribution to rainfall infiltration in soil slope. Electron J Geotech Eng. 2008;13 E(1999).

Acknowledgement
The author gratefully acknowledge the financial support provided by Fundamental Research Grant Scheme (FRGS) of Ministry of Education vot 4F853 from UTM and UNIMAS as for scholarship assistance throughout PhD study which had made the research project workable.